Probing the Two-Gate Mechanism of DNA Gyrase Using Cysteine Cross-Linking†

Nicola L. Williams and Anthony Maxwell*

Department of Biochemistry, University of Leicester, Leicester LE1 7RH, U.K.

Received June 2, 1999; Revised Manuscript Received July 19, 1999

ABSTRACT: Cross-linking a pair of novel cysteine residues on either side of the bottom dimer interface of DNA gyrase blocks catalytic supercoiling. Limited strand passage is allowed, but release of the transported DNA segment (T segment) via opening of the bottom dimer interface is prevented. In contrast, ATP-independent relaxation of negatively supercoiled DNA is completely abolished, suggesting that T-segment entry via the bottom gate is blocked. These findings support a two-gate model for supercoiling by DNA gyrase and suggest that relaxation by gyrase is the reverse of supercoiling. Cross-linking a truncated version of gyrase ($A64_2B_2$), which lacks the DNA wrapping domains, does not block ATP-dependent relaxation. This indicates that passage of DNA through the bottom dimer interface is not essential for this reaction. The mechanistic implications of these results are discussed.

DNA gyrase is a member of the family of type II DNA topoisomerases, a group of enzymes that catalyze the interconversion of different topological forms of DNA (*1*, *2*). These reactions are achieved by passing a segment of DNA (the "T" or "transported" segment) through another segment (the "G" or "gate" segment) that is held open by the enzyme.

Type II DNA topoisomerases are all structurally related and exist in their active conformations as dimers; each symmetry-related monomer is composed of one, two, or three subunits. Eukaryotic type II topoisomerases consist of a single pair of subunits. In contrast, bacterial DNA gyrase is composed of two pairs of subunits, A and B. The A subunit (GyrA;[1] 97 kDa) is homologous to the C-terminus of the eukaryotic enzymes, while the B subunit (GyrB; 90 kDa) is equivalent to the N-terminus (*3*). GyrB consists of two distinct domains: an N-terminal 43 kDa domain (GyrB43) and a C-terminal 47 kDa domain (GyrB47). Both domains have been cloned and can be expressed as separate gene products (*4*, *5*). GyrB43 is an ATPase domain, which dimerizes upon binding of ATP or the nonhydrolyzable ATP analogue, ADPNP (*4*, *6*). The crystal structure of this ATPase domain, complexed with ADPNP, has been determined (*7*). The N-terminal subdomains form dimer contacts constituting an ATP-operated clamp. There is no crystal structure currently available for GyrB47; however, the structure of an analogous domain within yeast DNA topoisomerase II (topo II) has been determined (*8*). This domain is proposed to interact with the GyrA subunits and play a role in DNA binding.

GyrA also consists of two domains: an N-terminal 64 kDa domain (GyrA64) and a C-terminal 33 kDa domain (GyrA33); both domains are available as separate gene products (*9*, *10*). The N-terminal domain contains the site of DNA breakage and reunion, and the crystal structure of a 59 kDa N-terminal fragment of this domain (GyrA59) has been determined (*11*). This structure is a dimer resembling a closed ring. The N-terminal head contains the active-site tyrosines involved in the DNA cleavage reaction, forming dimer contacts that constitute the DNA gate of the enzyme. The C-terminal tail also forms extensive dimer contacts. There is currently no structural information regarding the GyrA33 domains; however, it has been proposed that this domain, unique to gyrase, has a DNA-wrapping function (*10*, *12*). Two different crystal structure conformations of a 92 kDa fragment of yeast topo II, equivalent to GyrB47 and GyrA59, have also been determined (*8*, *13*), revealing another closed ring structure similar to GyrA59. In both cases, the DNA gate of yeast topo II is open, the top dimer contacts being provided by the N-terminal region that is analogous to GyrB47. Taken together, these structures of gyrase and topo II build up a picture of the whole type II topoisomerase enzyme: a dimeric structure with three dimer interfaces enclosing two interior cavities.

DNA gyrase is the target of a number of antibacterial agents (*14*), including the quinolones. These drugs work by stabilizing a cleavage complex between gyrase and DNA which, in vivo, leads to cell death, probably by blocking the passage of polymerases (*15*) and generating cytotoxic DNA breaks (*16*). In vitro, DNA cleavage by gyrase can be revealed if a reaction between gyrase, DNA, and a quinolone drug is terminated by the addition of SDS and proteinase K.

† This work was funded by the BBSRC. N.L.W. was supported by a CASE studentship funded by the BBSRC and Roche.

* To whom correspondence should be addressed. Telephone: +44 116 2523464. Fax: +44 116 2523630. E-mail: ony@leicester.ac.uk.

[1] Abbreviations: ADPNP, 5′-adenylyl β,γ-imidodiphosphate; GyrA, DNA gyrase A protein; GyrB, DNA gyrase B protein; GyrB43, N-terminal 43 kDa domain of GyrB; GyrB47, C-terminal 47 kDa domain of GyrB; GyrA64, N-terminal 64 kDa domain of GyrA; GyrA59, N-terminal 59 kDa fragment of GyrA; GyrA33, C-terminal 33 kDa domain of GyrA; A_2B_2, DNA gyrase tetramer; $A64_2A33_2B_2$, DNA gyrase reconstituted from GyrA64, GyrA33, and GyrB; $A64_2B_2$, truncated version of DNA gyrase reconstituted from GyrA64 and GyrB; DTT, dithiothreitol; PK/LDH, pyruvate kinase/lactate dehydrogenase; DiS, disulfide bond; PEP, phosphoenolpyruvate; SDS, sodium dodecyl sulfate; PAGE, polyacrylamide gel electrophoresis; $Cu(Phen)_3$, copper-(II)(1,10-phenanthroline)$_3$; BMH, 1,6-bismaleimidohexane; PDM, *N*,*N*′-*o*-phenylenedimaleimide; topo II, DNA topoisomerase II.

10.1021/bi9912488 CCC: $18.00
Published on Web 09/21/1999

It has also been found that Ca^{2+} can stabilize the cleavage of DNA by gyrase (*17*).

DNA gyrase is unique among type II topoisomerases in its ability to introduce negative supercoils into relaxed closed circular DNA. Other type II enzymes are unable to perform supercoiling, favoring relaxation instead. This preference is because conventional type II topoisomerases only bind a 25 bp region of DNA (*18*), relying on the topology of the DNA to present a T segment for capture. In contrast, DNA gyrase directs T-segment capture using the C-terminal DNA wrapping domains. It has been demonstrated that deletion of the C-terminal DNA wrapping domains gives rise to an enzyme that cannot supercoil DNA but relaxes DNA in an ATP-dependent manner (*12*).

DNA gyrase introduces negative supercoils into closed circular DNA by passing a segment of DNA through a transient break in a second segment. A section of DNA (the G segment) binds across the middle of the enzyme constituting the DNA gate. The DNA that is contiguous with the G segment is wrapped around the enzyme via the GyrA33 domains, presenting a second segment of DNA (the T segment) to the open ATP-operated clamp. The closure of the ATP-operated clamp is mediated by the binding of ATP or ADPNP, thus capturing a T segment (*19*). The cavity within the ATP-operated clamp is 20 Å wide and is just large enough to accommodate a single T segment (*7*). Double-stranded cleavage of the G segment and opening of the DNA gate then allows the T segment to pass through into the bottom cavity. Closing of the DNA gate and religation of the G segment can then occur. To complete enzyme turnover, the ATP-operated clamp reopens after ATP hydrolysis and the T segment must exit from the enzyme.

Until recently, the mode of exit of the T segment after strand passage has been uncertain. However, evidence now suggests that the T segment exits yeast topo II through an open C-terminal dimer interface at the bottom of the enzyme. Binding of ADPNP can lead to decatenation of a singly linked catenane by yeast topo II. The ring containing the G segment remains associated with the enzyme, but the DNA ring containing the T segment is found to be free in solution (*20*). Since the ATP-operated clamp is apparently irreversibly closed upon binding of ADPNP, this indirectly implies that the T segment must exit via the bottom dimer interface. However, the possibility that T-segment release occurs before ADPNP fully closes the ATP-operated clamp or that terminating the reaction artificially releases the T segment cannot be ruled out. More direct evidence has since been obtained by locking the bottom dimer interface of yeast topo II using a disulfide bridge (*21*). Cysteine residues have been introduced across the dimer interface using the crystal structure of the 92 kDa fragment of yeast topo II as a guide (*8*). The ADPNP-induced single-step decatenation experiments were reproduced. With the bottom dimer interface locked by a disulfide bridge, decatenation could still occur; however, the ring containing the T segment now remained topologically linked to the enzyme. This ring could be subsequently released from the enzyme by reduction of the disulfide bridge. The ATP-dependent relaxation activity of yeast topo II was also tested. The un-cross-linked enzyme could perform multiple rounds of relaxation in the presence of ATP. In contrast, the cross-linked enzyme could only perform a single relaxation event per enzyme. These experiments provide strong evidence supporting the two-gate model for eukaryotic type II DNA topoisomerases, in which the T segment enters via the ATP-operated clamp and exits via the bottom gate.

Despite this evidence, the matter remains in contention. Another group has shown that a truncated version of yeast topo II, intradimerically tethered at the C-terminus, is catalytically active in DNA transport (*22*). However, the location of the tether cannot be mapped onto the 92 kDa crystal structure of yeast topo II, making interpretation difficult. In addition, the flexible tether may be long enough to support multiple rounds of strand passage and T-segment release. In an attempt to further clarify the route of T-segment exit, we have investigated the role of the bottom dimer interface using an alternative type II topoisomerase, DNA gyrase.

Although yeast topo II has proven to be a useful model for most type II DNA topoisomerases, DNA gyrase is distinct from yeast topo II in a number of ways. These important distinctions mean it is necessary to probe directly the role of the bottom dimer interface of gyrase. First, gyrase is unique in this class since it is the only type II enzyme that is able to introduce negative supercoils into closed circular DNA. This unique ability is attributed to the wrapping of the DNA that is contiguous to the G segment, such that the ends are presented as possible T segments. Second, gyrase is active as an A_2B_2 tetramer, whereas yeast topo II is a homodimer. This means that dissociation between the A and B subunits is possible for gyrase, but impossible for yeast topo II. Opening of this A−B interface may provide the exit route for the T segment in the case of gyrase. Third, gyrase is the only enzyme in this class that is able to perform an ATP-independent form of relaxation. This raises the question of whether the T segment passes through the bottom dimer interface during relaxation. In this paper, we analyze the role of the bottom dimer interface of DNA gyrase by cross-linking it using disulfide bond formation and two cysteine-specific cross-linking reagents. The effects on both supercoiling and relaxation are discussed.

EXPERIMENTAL PROCEDURES

Materials. 1,10-Phenanthroline and PDM were purchased from Sigma. DTT was from Melford Laboratories. BMH was from Pierce. *Escherichia coli* MAX Efficiency DH5αF′IQ competent cells were from Gibco BRL. DNA oligonucleotides used for site-directed mutagenesis and sequencing were obtained from PNACL (Leicester University). Negatively supercoiled and relaxed forms of plasmid pBR322 were gifts from A. J. Howells (University of Leicester). Wild-type GyrB (gift from A. J. Howells, University of Leicester), GyrA64, GyrA33, and GyrA were purified as described previously (*9*, *10*, *23*), except that GyrA64 was expressed in *E. coli* DH5αF′IQ cells.

Site-Directed Mutagenesis. Amino acid changes within GyrA or GyrA64 were introduced by site-directed mutagenesis of plasmid pPH3 (*23*) or pRJR242 (*9*) using QuikChange (Stratagene). Successful mutagenesis was confirmed by DNA sequence analysis which was performed by PNACL (University of Leicester).

Disulfide Bond Formation. GyrA or GyrA64 (20 μM) was reduced in the presence of 40 mM DTT in enzyme buffer

[50 mM Tris-HCl (pH 7.5), 10% (w/v) glycerol, 1 mM EDTA, 4 mM DTT, and 100 mM KCl] for 1 h at 37 °C, followed by removal of DTT and EDTA by gel filtration (Nick spin columns, Pharmacia) or extensive dialysis against TGK buffer [50 mM Tris-HCl (pH 7.5), 10% (w/v) glycerol, and 100 mM KCl]. Oxidation by ambient oxygen was performed using the redox catalyst Cu(II)(1,10-phenanthroline)$_3$ (125 μM) during a 1 h incubation at 37 °C with the enzyme (10 μM), prior to quenching with 1 mM EDTA. [Cu(Phen)$_3$ was prepared by adding a 3-fold excess of 1,10-phenanthroline to $CuSO_4$.]

Disulfide Bond Reduction. Disulfide bonds formed across the bottom dimer interface of GyrA64 were broken by reduction with DTT. GyrA64$^{C194A/R462C}$ (10 μM) was incubated in enzyme buffer containing 40 mM DTT for 1 h at 37 °C.

Use of Cross-Linking Reagents. GyrA or GyrA64 (20 μM) was reduced in the presence of 40 mM DTT in enzyme buffer for 1 h at 37 °C. Buffer was exchanged by gel filtration (Nick spin columns, Pharmacia) with enzyme buffer without DTT. PDM or BMH (dissolved in acetonitrile) was added to GyrA or GyrA64 (10 μM) to give a final cross-linker concentration of 25 μM and 1% acetonitrile prior to incubation for 1 h at 37 °C. Cross-linking was quenched by the addition of 4 mM DTT.

Gel Purification, Electroelution, and Refolding. GyrA64 (500 μg) cross-linked via a disulfide bond, PDM or BMH, was prepared as described above. Samples were prepared for SDS−PAGE by the addition of an equal volume of 125 mM Tris-HCl (pH 6.8), 4% (w/v) SDS, 20% (w/v) glycerol, and 0.002% bromophenol blue with or without 10% β-mercaptoethanol as appropriate, and then the mixtures were boiled for 5 min. Denatured samples were loaded onto a 1.5 mm thick, 7.5% discontinuous polyacrylamide preparative gel containing 0.1% SDS with a 4% polyacrylamide stacking gel. Gels were run in SDS running buffer [25 mM Tris, 192 mM glycine, and 0.1% (w/v) SDS] using a Mini-Protean II gel system (Bio-Rad) until the dye front reached the bottom of the gel. Temporary visualization of the bands was achieved by soaking the gel in 0.25 M KCl for 5 min. After excision of the required band, the gel slice was placed inside a length of dialysis tubing (10 kDa molecular mass cutoff) containing 5 mL of SDS running buffer. The bag was sealed at both ends, taking care not to trap air inside. It was then placed into a horizontal gel electrophoresis tank filled with SDS running buffer and electrophoresed at 100 V for 2 h before reversing the voltage for 5 min. The sample was dialyzed extensively against 2 M urea prior to the removal of the gel slice. The protein solution was concentrated to 100 μL (using a Centricon-10 concentrator, Amicon). Protein refolding was achieved as described previously (*17*) by dilution with 4 mL of enzyme buffer containing 9 M urea, prior to extensive dialysis against enzyme buffer.

Enzyme Assays. Supercoiling assays were performed as previously described (*17*) except that the concentrations of spermidine, KCl, $MgCl_2$, and relaxed pBR322 were increased to 5 mM, 30 mM, 8 mM, and 7.2 nM, respectively. ATP-independent relaxation was carried out as described for supercoiling, except that ATP and spermidine were omitted, the $MgCl_2$ concentration was increased to 16 mM, and negatively supercoiled pBR322 replaced relaxed pBR322. ATP-dependent relaxation was carried out as described for supercoiling, except GyrA33 and spermidine were omitted and negatively supercoiled pBR322 replaced relaxed pBR322. Quinolone-stabilized cleavage assays were carried out as described for ATP-dependent relaxation, except that ATP was omitted and 50 μM ciprofloxacin (CFX) was added. Ca^{2+}-stabilized cleavage assays were performed exactly as described for quinolone-stabilized cleavage except that 4 mM $CaCl_2$ replaced $MgCl_2$ and the quinolone drug was not included. All reactions were terminated by the addition of SDS to a final concentration of 0.2% and proteinase K to a final concentration of 0.1 mg/mL and incubation for 30 min at 37 °C. Samples were prepared for electrophoresis by the addition of 0.5 volume of 100 mM Tris-HCl (pH 7.5), 40% (w/v) sucrose, 1 mM EDTA, 0.002% bromophenol blue, and an equal volume of chloroform/isoamyl alcohol (24/1) and extensively mixed by vortexing. The aqueous layer was analyzed using 1% agarose gels in 40 mM Tris-acetate and 2 mM EDTA for either 4 h at 90 V or 16 h at 45 V. The DNA was then visualized by staining with ethidium bromide (1 μg/mL). To resolve the distribution of negatively supercoiled topoisomers, chloroquine (20 μg/mL) was present in the gel and running buffer. ATPase assays were performed using the PK/LDH linked assay as described previously (*4*) except that the concentration of KCl was reduced to 30 mM and the concentrations of PEP and NADH were increased to 800 and 400 μM, respectively. Linear pBR322 (5 nM) was used where indicated. Reactions were initiated by adding ATP (2 mM). In all procedures described above involving proteins cross-linked via a disulfide bond, DTT was omitted. If appropriate, DTT was also removed from buffers containing GyrB and GyrA33 by gel filtration (Nick spin columns, Pharmacia) immediately prior to use.

RESULTS

Design and Properties of the Bottom Gate Mutants. The crystal structure of the 59 kDa fragment of GyrA (*11*) was examined so that a range of mutants to be cross-linked could be designed. Cysteine residues were introduced, using site-directed mutagenesis, on either side of the bottom dimer interface of GyrA (Figure 1). Detailed analysis of disulfide bonds within proteins with known crystal structures shows that disulfide bridges can adopt a wide range of conformations and cross-link most forms of secondary structure (*24*, *25*). In most cases, S−S disulfide bond distances are 2−3 Å, with Cβ−Cβ separations of 4−5 Å. To favor disulfide bond formation within GyrA, the locations of the novel cysteine residues were chosen such that Cβ−Cβ distances would not exceed 6 Å. This led to the construction of four GyrA mutants (Table 1). These were tested for activity prior to disulfide bond formation, in the presence of 4 mM DTT. This included supercoiling, ATP-independent relaxation, and quinolone- and Ca^{2+}-stabilized cleavage. Two mutants (GyrA^{R462C} and GyrA$^{L459C/Q464C}$) exhibit characteristics matching those of wild-type GyrA. GyrA$^{I397C/L466C}$ exhibited reduced activity, and GyrA$^{L461C/L463C}$ was inactive (Table 1).

Cross-Linking the Bottom Dimer Interface of DNA Gyrase via Disulfide Bond Formation. To promote disulfide bond formation, the reducing agent (DTT) was removed by gel filtration or dialysis. The formation of intersubunit disulfide cross-links was assessed using nonreducing SDS−PAGE, in which the protein is denatured but any disulfide cross-links

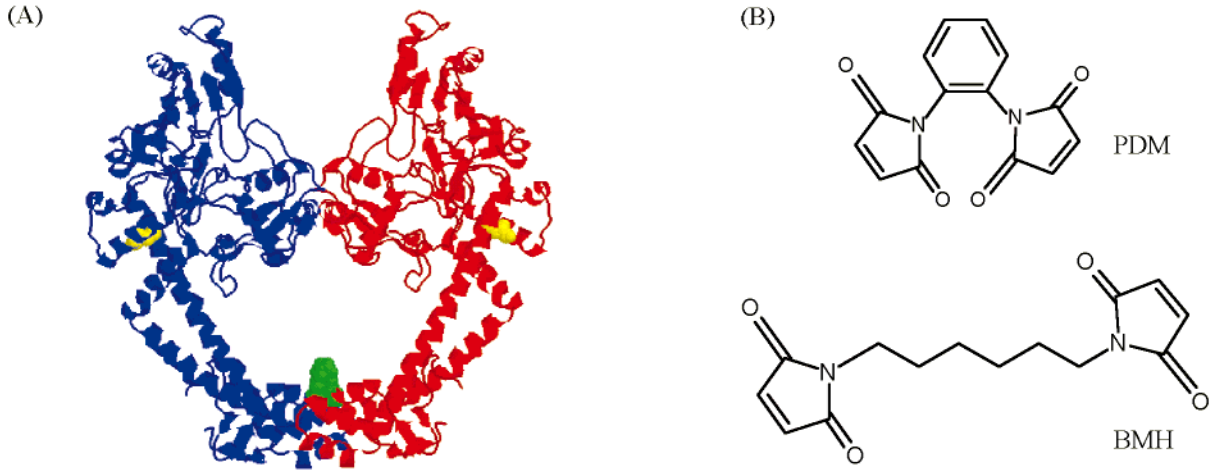

FIGURE 1: (A) Ribbon representation of the crystal structure of the GyrA59 dimer (*11*). Each monomer is colored red or blue, and the locations of the Arg[462] to Cys and Cys[194] to Ala mutations are shown as green and yellow space-filling representations, respectively. (B) Structures of *N*,*N*′-*o*-phenylenedimaleimide (PDM) and 1,6-bismaleimidohexane (BMH).

Table 1: Activities of Mutant Proteins

	GyrA	GyrA	GyrA	GyrA	GyrA64	GyrA64
amino acid mutations[a]	R462C	L459C Q464C	I397C L466C	L461C L463C	C194A	C194A R462C
supercoiling and ATP-independent relaxation activity of gyrase (%)[b]	100	100	30	0	100	100
ATP-dependent relaxation activity of $A64_2B_2$ compared to that of the wild type (%)	N/A[c]	N/A	N/A	N/A	100	100
quinolone- and Ca^{2+}-stimulated cleavage compared to that of the wild type (%)	100	100	N/T[d]	N/T	N/T	100

[a] The R462C mutation was designed for disulfide bond formation with its opposite number across the dimer interface; others required double mutations in each subunit for the possible formation of two disulfide cross-links. [b] Under reducing conditions, GyrA mutants were compared with wild-type GyrA, and GyrA64 mutants were compared with wild-type GyrA64 in the presence of GyrA33. [c] Not applicable. [d] Not tested.

remain intact. None of the four GyrA mutants was found to spontaneously form intersubunit disulfide bridges specifically across the bottom dimer interface. In contrast, the addition of a mild oxidizing reagent, copper(II) phenanthroline, caused unwanted disulfide bond formation between native cysteine residues, resulting in multimerization of GyrA (data not shown). For exclusive disulfide bond formation between the novel cysteine residues, it was evident that the four native cysteines within GyrA must not be exposed to the oxidizing agent. This was achieved by introducing the novel cysteines into the 64 kDa fragment of GyrA (GyrA64). This domain only contains one native cysteine residue (Cys[194]) which was replaced with alanine (Figure 1). The Arg[462] to Cys mutation was made within GyrA64 because full-length GyrA bearing this mutation had previously been shown to exhibit wild-type characteristics (Table 1) and only a single mutation is required. It has been shown that reconstitution of GyrA64, GyrA33, and GyrB gives rise to an enzyme capable of catalyzing DNA supercoiling (*10*), although at a reduced level compared with that of intact gyrase (A_2B_2). We found that the reconstituted complex ($A64_2A33_2B_2$) had a supercoiling activity approximately 10-fold lower than that of intact gyrase (data not shown). Characterization of both GyrA64^{C194A} and GyrA64$^{C194A/R462C}$, under reducing conditions, confirmed that the introduction of the two mutations, Arg[462] to Cys and Cys[194] to Ala, into GyrA64 did not affect the supercoiling activity of $A64_2A33_2B_2$ (Table 1).

Spontaneous disulfide bond formation did not occur in GyrA64$^{C194A/R462C}$ following the removal of the reducing agent. However, mild oxidation of GyrA64$^{C194A/R462C}$ catalyzed by copper(II) phenanthroline produced approximately 90% conversion into intersubunit cross-linked GyrA64 dimers (Figure 2). More than one band is observed for cross-linked GyrA64, representing a range of SDS-bound conformations with differing mobilities; these do not necessarily reflect the native conformation of the cross-linked protein in solution. Separation of cross-linked and un-cross-linked GyrA64 was not possible using gel filtration under native

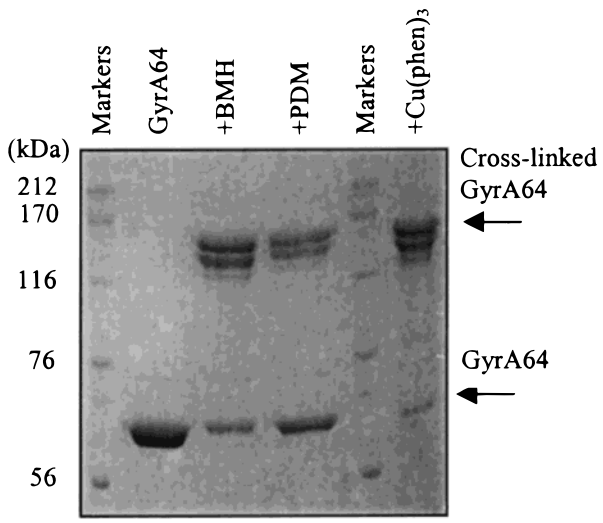

FIGURE 2: SDS−PAGE analysis of cross-linked GyrA64. GyrA64$^{C194A/R462C}$ (10 μM) was incubated under nonreducing conditions alone or in the presence of BMH (25 μM) or PDM (25 μM) for 1 h at 37 °C. Reactions were quenched with DTT (4 mM) and the mixtures analyzed by SDS−PAGE. Disulfide cross-links were formed by incubating GyrA64$^{C194A/R462C}$ (10 μM) under nonreducing conditions in the presence of copper(II) phenanthroline (125 μM). The reaction was quenched with EDTA (1 mM) and the mixture analyzed by SDS−PAGE under nonreducing conditions.

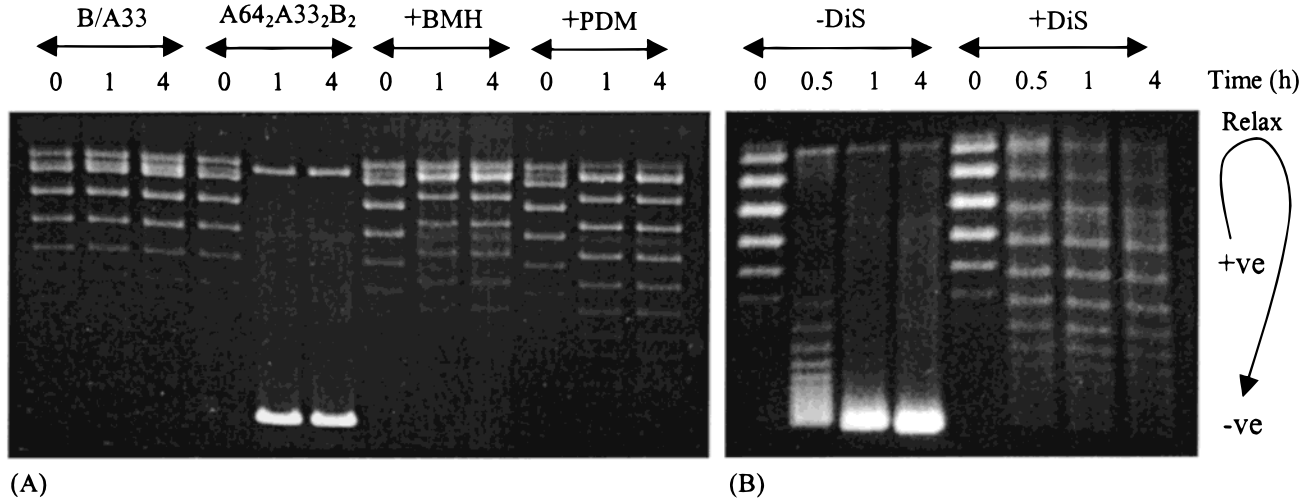

FIGURE 3: Time course of supercoiling by A64$_2$A33$_2$B$_2$ cross-linked via BMH, PDM, or disulfide bond formation. (A) Relaxed pBR322 (7.2 nM) was incubated with GyrA33 (300 nM) and GyrB (600 nM) alone, with GyrA64$^{C194A/R462C}$ (300 nM), or with BMH cross-linked or PDM cross-linked GyrA64$^{C194A/R462C}$ (gel purified, 300 nM) in the presence of 1.4 mM ATP and 4 mM DTT at 37 °C for the indicated periods of time. (B) Relaxed pBR322 (7.2 nM) was incubated with GyrA33 (200 nM), GyrB (400 nM), and disulfide cross-linked GyrA64 (100 nM, gel purified, reduced or nonreduced) in the presence of 1.4 mM ATP with or without 4 mM DTT at 37 °C for the indicated periods of time. Samples were analyzed on 1% agarose gels. Relaxed pBR322 appears slightly positive on the agarose gel; the arrow on the right indicates the expected shift in mobility following supercoiling by gyrase (positions of positive and negative topoisomer bands are staggered with respect to each other).

conditions, since GyrA64 was found to exist as a dimer in solution (data not shown). Instead, cross-linked GyrA64 was separated from un-cross-linked GyrA64 and any contaminating GyrA under denaturing conditions using preparative SDS−PAGE. The cross-linked band was excised and electroeluted. The sample was then fully denatured in the presence of urea and allowed to refold following the removal of urea by dialysis. Similar gel purification and refolding of un-cross-linked GyrA64$^{C194A/R462C}$ was shown not to affect activity (data not shown). The cross-links could be broken by incubation with 40 mM DTT, indicating that they were disulfide bonds. Incubation of wild-type GyrA64 under identical oxidizing conditions gave no intersubunit cross-linking, confirming that the intersubunit cross-linking in GyrA64$^{C194A/R462C}$ must be due to disulfide bond formation between the symmetry-related pair of Cys^{462} residues across the bottom dimer interface (data not shown).

Cross-Linking the Bottom Dimer Interface of DNA Gyrase Using Long and Short Cross-Linking Reagents. The disulfide bond is a cross-linker which effectively locks the bottom dimer interface in the closed position. It is possible that restricting the conformational flexibility of the bottom dimer interface in this way may block other essential conformational changes within the enzyme. This concern was addressed by using two cysteine-specific, irreversible cross-linking reagents (BMH and PDM) of different sizes to allow some conformational freedom at the bottom dimer interface. Both contain two maleimide functional groups either separated by a C_6 spacer (∼16 Å long) or on adjacent carbons of a phenyl ring (∼4 Å) (Figure 1). Incubation of GyrA^{R462C} with BMH or PDM under nonreducing conditions and subsequent analysis on SDS−PAGE shows the conversion of GyrA into a range of high-molecular mass species. Once again, this suggests cross-linking involving the native cysteine residues within GyrA. In contrast, incubation of GyrA64$^{C194A/R462C}$ with the long cross-linker BMH or the short cross-linker PDM results in ∼80 or ∼50% conversion into cross-linked GyrA64 dimers, respectively (Figure 2). Several dimer conformations were observed for the cross-linked products. Incubation of wild-type GyrA64 with either BMH or PDM gives rise to no cross-linked product (data not shown), indicating that the intersubunit cross-linking exhibited by GyrA64$^{C194A/R462C}$ can be attributed to cross-linking between the novel pair of cysteine residues at the bottom dimer interface. The BMH and PDM cross-linked GyrA64 dimers were gel purified and refolded, as described above, to remove any un-cross-linked GyrA64 or GyrA contamination.

Catalytic Supercoiling Is Blocked by Locking the Bottom Dimer Interface of DNA Gyrase. Cross-linking the bottom dimer interface of GyrA64$^{C194A/R462C}$ via a disulfide bond or the irreversible cross-linking reagent BMH or PDM prior to reconstitution with GyrA33 and GyrB inhibits supercoiling activity (Figure 3). However, upon reduction of the disulfide bond, by incubation with 40 mM DTT, full supercoiling activity is restored. To maintain the disulfide bond, DTT is not present in the disulfide cross-linked supercoiling assay, in contrast to the un-cross-linked sample which contains 4 mM DTT. However, the observed loss in activity exhibited by the disulfide cross-linked enzyme cannot be ascribed to the absence of DTT. The supercoiling and ATP-independent relaxation activities of A64$_2$A33$_2$B$_2$ were found to be reduced by a factor of only 2 in the absence of DTT compared with the activity in the presence of 4 mM DTT (data not shown).

Although supercoiling is inhibited by cross-linking the bottom dimer interface of gyrase, it is not completely abolished. The distribution of relaxed topoisomers (running slightly positive on the agarose gel) is shifted in the direction of negatively supercoiled product after incubation with cross-linked gyrase and ATP (Figure 3). This is observed for all three types of cross-linkers. The average change in topoisomer linking number per enzyme (ΔLk/enz) exhibited by gyrase cross-linked using a disulfide bond, PDM, or BMH is −0.86, −0.24, or −0.14, respectively (Figure 3 and Table 2). Since a single round of supercoiling by gyrase results in a ΔLk/enz of −2, this reflects a substoichiometric level of

Table 2: Comparison of the Properties of $A64_2A33_2B_2$ and $A64_2B_2$ with or without Cross-Linkers

$A64_2A33_2B_2$[a]	un-cross-linked	with DiS	with PDM	with BMH
supercoiling ($-\Delta$Lk/enz)[b]	>2	0.86	0.24	0.14
ATP-independent relaxation	100%	none	none	none
quinolone-stabilized cleavage	100%	N/T[c]	60%	60%
Ca^{2+}-stabilized cleavage	100%	N/T	60%	60%
ATPase rate (s^{-1})[d] without DNA	0.131	0.091	0.128	0.125
ATPase rate (s^{-1})[d] with DNA	0.317	0.162	0.285	0.263

$A64_2B_2$[a]	un-cross-linked	with DiS	with PDM	with BMH
ATP-dependent relaxation (ΔLk/enz)	2.7	3.2	3.0	3.0
quinolone-stabilized cleavage	100%	N/T	100%	100%
Ca^{2+}-stabilized cleavage	100%	N/T	N/T	100%

[a] $GyrA64^{C194A/R462C}$ was used. [b] ΔLk/enz represents the change in linking number per enzyme between the most intense topoisomers at time zero and after 4 h. [c] Not tested. [d] GyrB (50 nM) was incubated with GyrA64 (with or without cross-linker, 100 nM) and GyrA33 (100 nM) in the presence or absence of linear pBR322 (5 nM).

strand passage. In addition, the maximum level of supercoiling does not increase with time, suggesting that enzyme turnover is blocked by the presence of the cross-linkers. In contrast, the maximum level of supercoiling exhibited by un-cross-linked gyrase does increase with time and represents a ΔLk/enz exceeding -2. This indicates that gyrase can perform multiple rounds of strand passage in the absence of the cross-linker.

ATP-Independent Relaxation Is Blocked by Cross-Linking the Bottom Dimer Interface of Gyrase. Cross-linking the bottom dimer interface of gyrase abolishes the ATP-independent relaxation of negatively supercoiled DNA. This can be observed using all three types of cross-linkers. Figure 4 shows that full relaxation is achieved by gyrase within 1 h; however, there are no signs of relaxation by the cross-linked gyrase after incubation for 4 h. This suggests that in the absence of ATP, cross-linked gyrase cannot perform strand passage. This is in contrast to the strand passage exhibited by cross-linked gyrase in the presence of ATP. The inability to perform even a single strand passage event in the absence of ATP suggests that, for ATP-independent relaxation by gyrase, a T segment enters through opening of the bottom dimer interface. Once the T segment is within the bottom cavity, this may lead to energetically favorable strand passage through a transient break in the G segment and exit through the open ATP-operated clamp. Cross-linking the bottom dimer interface of gyrase prevents entry of the T segment; hence, no strand passage is observed.

Locking the Bottom Gate Does Not Block ATP-Dependent Relaxation by the $A64_2B_2$ Complex. A truncated version of gyrase lacking the C-terminal DNA wrapping domains ($A64_2B_2$) has been shown to lack supercoiling activity, but is capable of ATP-dependent relaxation (*12*). However, $A64_2B_2$ exhibits a distributive form of relaxation in contrast

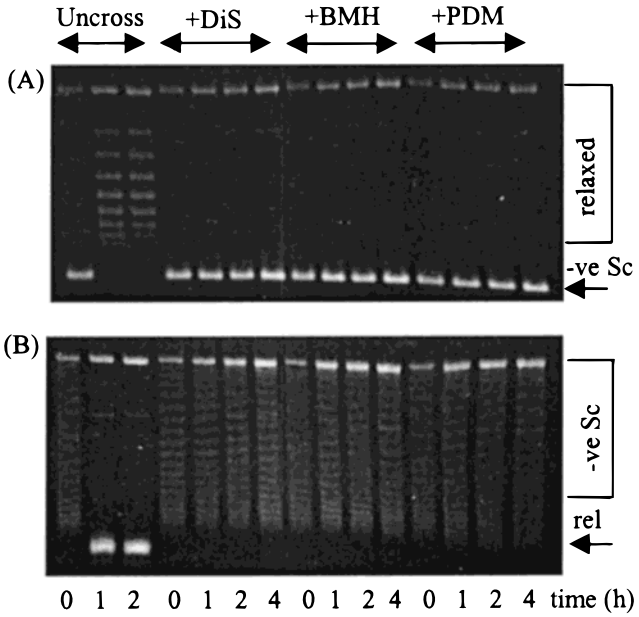

FIGURE 4: Time course of ATP-independent relaxation by $A64_2A33_2B_2$ cross-linked via BMH, PDM, or disulfide bond formation. Negatively supercoiled pBR322 (7.2 nM) was incubated with GyrA33 (300 nM), GyrB (500 nM), and disulfide cross-linked GyrA64 (300 nM, gel purified, reduced or nonreduced) or GyrA64 cross-linked using BMH or PDM (gel purified, 300 nM) at 37 °C for the indicated periods of time. Samples were analyzed on a 1% agarose gel (A) or a 1% agarose gel containing 20 μg/mL chloroquine (B). In the presence of chloroquine, relaxed DNA appears positively supercoiled, whereas negatively supercoiled DNA appears relaxed.

to the processive supercoiling of gyrase. This possibly reflects the inherent instability of the $A64_2B_2$ complex in the absence of the GyrA33 domains. We have found that this complex is also unable to perform ATP-independent relaxation (data not shown). These characteristics are analogous to those of other conventional type II topoisomerases.

The $A64_2B_2$ complex cross-linked across the bottom dimer interface with BMH, PDM, or disulfide bond formation has been found to retain full ATP-dependent relaxation activity (Figure 5). In fact, the extent of relaxation exhibited by the complex is increased in the presence of the cross-linkers. These findings indicate that opening of the bottom dimer interface is not essential for the exit of the T segment after strand passage. This is in direct contrast to the case for the ATP-dependent relaxation mechanism of yeast topo II (*21*). These results also establish that the T segment does not enter through the bottom dimer interface, unlike the relaxation mechanism of full-length gyrase.

Locking the Bottom Gate of DNA Gyrase Does Not Block Quinolone- or Ca^{2+}-Stabilized Cleavage. During the DNA supercoiling reaction, DNA gyrase catalyzes the transient double-stranded cleavage of a bound G segment. This transient cleavage can be stabilized in the presence of quinolone drugs or if $MgCl_2$ is replaced with $CaCl_2$. These cleavage reactions can also be performed by the truncated version of DNA gyrase ($A64_2B_2$) lacking the C-terminal DNA wrapping domains (*9*, *12*). This shows that the binding and cleavage of the G segment does not necessarily require the wrapping of the DNA around the enzyme.

Cross-linking the bottom dimer interface does not affect the ability of $A64_2B_2$ to carry out DNA cleavage; both

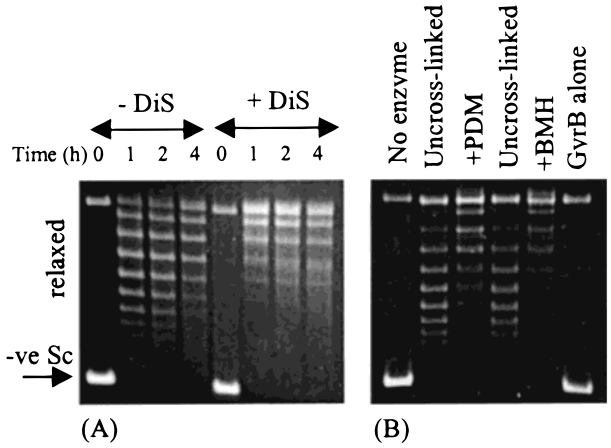

FIGURE 5: ATP-dependent relaxation by cross-linked $A64_2B_2$. (A) Negatively supercoiled pBR322 (7.2 nM) was incubated with GyrB (800 nM) and disulfide cross-linked GyrA64 (200 nM, gel purified, reduced or nonreduced) in the presence of 1.4 mM ATP with or without 4 mM DTT at 37 °C for the indicated periods of time. (B) Negatively supercoiled pBR322 (7.2 nM) was incubated with GyrB (800 nM) alone, with $GyrA64^{C194A/R462C}$ (200 nM), or with BMH cross-linked or PDM cross-linked GyrA64 (200 nM, gel purified) in the presence of ATP (1.4 mM) and DTT (4 mM) at 37 °C for 1 h. Samples were analyzed on 1% agarose gels.

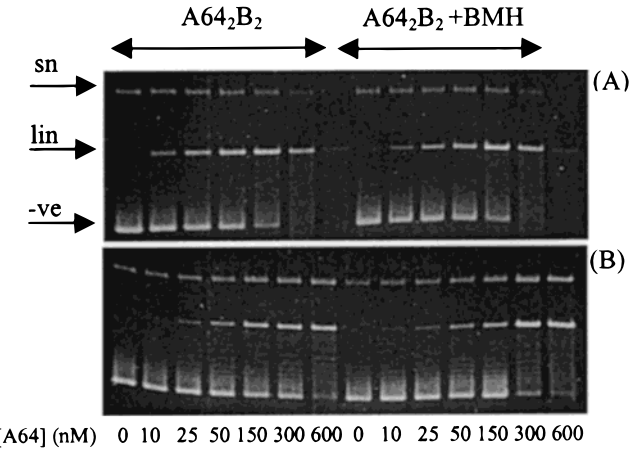

FIGURE 6: Quinolone- and Ca^{2+}-stabilized cleavage by $A64_2B_2$ (with or without BMH). Negatively supercoiled pBR322 (3.6 nM) was incubated with $GyrA64^{C194A/R462C}$ (concentrations indicated) or $GyrA64^{C194A/R462C}$ cross-linked with BMH (gel purified, concentrations indicated) and a 2-fold excess of GyrB in the presence of (A) ciprofloxacin (50 μM) or (B) $CaCl_2$ (4 mM) at 37 °C for 1 h. Reactions were terminated by adding 0.2% SDS and 0.1 mg/mL proteinase K. Samples were analyzed on 1% agarose gels (sn, singly nicked; lin, linear; and −ve, negatively supercoiled).

quinolone- and Ca^{2+}-stabilized cleavage reactions are seen to occur (Figure 6 and Table 2). The $A64_2A33_2B_2$ complex tethered across the bottom dimer interface can also exhibit DNA cleavage, albeit at a reduced level compared with that of the un-cross-linked complex (Table 2). These results suggest that cross-linking the bottom dimer interface of gyrase does not prevent binding and cleavage of the G segment or binding of quinolone drugs.

Locking the Bottom Gate of DNA Gyrase Does Not Prevent DNA Stimulation of ATP Hydrolysis. DNA gyrase exhibits a low level ATPase activity, which is stimulated in the presence of DNA, dependent on the length of the DNA (*26*). A segment of DNA that is >100 bp is required to stimulate the ATPase rate; short segments cannot unless present at high concentrations. A mutation inside the ATP-operated clamp of GyrB (Arg^{286} to Gln) has also been shown to block DNA stimulation of the ATPase (*27*). Together, these results imply that the T segment must be captured by the ATP-operated clamp to stimulate ATP hydrolysis. Consequently, the ability to perform DNA-stimulated ATPase indicates whether the DNA is wrapped and the T segment is presented to the ATP-operated clamp ready for strand passage. We have found that cross-linking the bottom dimer interface of the $A64_2A33_2B_2$ complex does not block DNA stimulation of ATP hydrolysis (Table 2). This suggests that ATP hydrolysis and presentation of the T segment to the ATP-operated clamp are not perturbed by cross-linking of the bottom dimer interface. The level of ATP hydrolysis observed in the presence of DNA is low compared to that observed previously for gyrase (*26*). However, this may reflect the inherent instability of $A64_2A33_2B_2$ compared with A_2B_2.

DISCUSSION

Using the crystal structure of the 59 kDa N-terminal fragment of the DNA gyrase A protein as a guide, we have introduced novel cysteine residues on either side of the bottom dimer interface of GyrA. However, selective cross-linking of the novel cysteines was not possible due to the reactivity of the four native cysteine residues in GyrA. To overcome this problem, a novel cysteine (Arg^{462} to Cys) was introduced into the N-terminal 64 kDa fragment of GyrA (GyrA64), and the single native cysteine within this domain was replaced with alanine (Cys^{194} to Ala). The bottom dimer interface of GyrA64 was cross-linked using long or short cysteine-specific cross-linking reagents or via disulfide bond formation. This enabled reconstitution of cross-linked gyrase by the addition of GyrA33 and GyrB to GyrA64 to generate the $A64_2A33_2B_2$ complex.

Locking the Bottom Gate Blocks Catalytic Supercoiling by Preventing T-Segment Release after Strand Passage. DNA supercoiling by gyrase involves the capture of a T segment by the ATP-operated clamp. This leads to a conformational cascade in which the T segment may be passed through a transient break in the G segment and into the bottom cavity. The bottom cavity is likely only to be large enough to accommodate a single DNA duplex (*11*); hence, T-segment exit would normally be required prior to the next round of strand passage. Exit may occur either via opening of the bottom dimer interface or via dissociation of the A and B subunits. To distinguish between these two possibilities, we have locked the bottom dimer interface of gyrase.

We have shown that cross-linked gyrase can capture a T segment and pass it through a transient break in the G segment and into the bottom cavity. However, enzyme turnover is blocked, suggesting that the T segment normally exits via opening of the bottom dimer interface (Figure 7). When T-segment release through the bottom gate of gyrase is restricted by a cross-linker, further rounds of strand passage are not possible since it is likely that only one T segment can occupy the bottom cavity at any one time (*11*). Hence, ΔLk/enz does not exceed −2 in the presence of the cross-linker.

Incubation of relaxed pBR322 with disulfide cross-linked gyrase produces a range of negatively supercoiled topoisomers. The average level of supercoiling represents single-

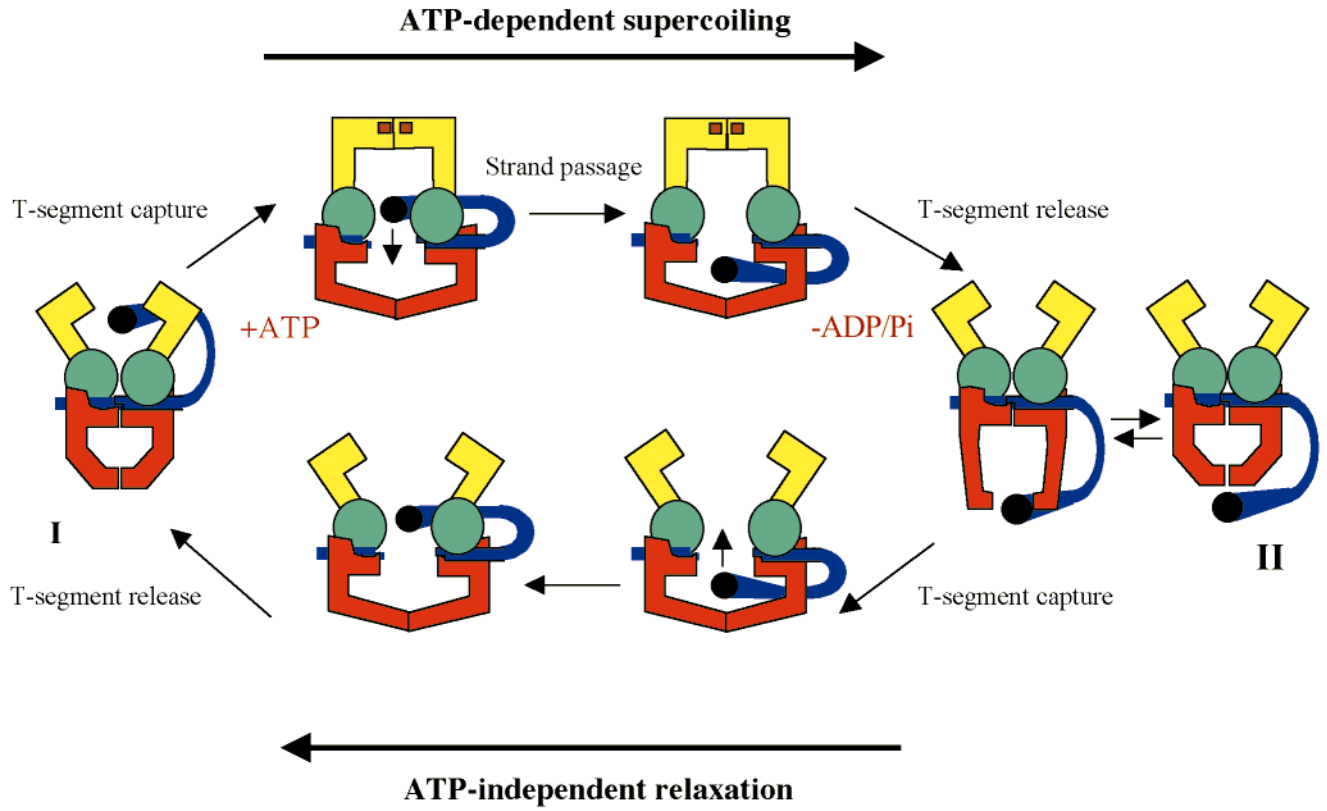

FIGURE 7: Combined two-gate model of supercoiling and relaxation by DNA gyrase. Gyrase is shown bound to DNA (GyrA64, red; GyrB47, green; GyrB43, yellow; ATP, brown; and DNA, blue); for simplicity, the two GyrA33 domains and one arm of the wrapped T segment are not shown. DNA is wrapped around gyrase such that a T segment is presented to the ATP-operated clamp (I) or the bottom gate (II). In the presence of ATP, T-segment capture occurs via dimerization of the ATP-operated clamp. This leads to strand passage and T-segment release via the bottom gate. This route is favored by positively supercoiled and relaxed DNA substrate. In the absence of ATP, T-segment capture via opening of the bottom gate predominates. This leads to reverse strand passage and T-segment release via the open ATP-operated clamp. This route is favored by negatively supercoiled DNA.

cycle strand passage by ~40% of the disulfide cross-linked population. This is an unexpectedly high level of strand passage; the efficiency of ADPNP-driven strand passage of relaxed DNA by gyrase is normally only ~25% (*28*, *29*). Locking the ATP-operated clamp with ADPNP or cross-linking the bottom gate both blocks enzyme turnover. However, we suggest that a higher efficiency of strand passage is observed with the cross-linker because the use of ATP allows multiple rounds of T-segment capture. This enables cross-linked gyrase to have multiple attempts at passing a T segment into the bottom cavity, increasing the overall efficiency. Despite this, stoichiometric strand passage is not observed, suggesting that the T segment is not stable in the bottom cavity. Since the T segment cannot exit via the bottom gate, strand passage must be reversible, enabling the T segment to pass back up through the G segment. The T segment may then exit via the ATP-operated clamp that has reopened after ATP hydrolysis, resulting in no net strand passage. However, reversal of strand passage may be temporarily blocked if a second T segment is captured in the ATP-operated clamp first. In this case, both the top and bottom cavities would be occupied, preventing strand passage in any direction. The supercoiling observed upon termination of the reaction may represent the populations of cross-linked gyrase transiently bound to one or two T segments.

The low level of strand passage exhibited by cross-linked gyrase is different from that observed for yeast topo II. Cross-linking the bottom gate of yeast topo II enabled a single round of decatenation or relaxation to be performed per enzyme (*21*); reversal of strand passage was not observed. This highlights a fundamental difference between yeast topo II and gyrase; i.e., strand passage by yeast topo II is strictly unidirectional and ATP-driven. In contrast, gyrase can perform bidirectional strand passage that does not necessarily require ATP.

The type of cross-linker also affects the level of supercoiling. Gyrase cross-linked with BMH and PDM exhibits only 7 and 12% strand passage efficiency, respectively. This is significantly lower than the 40% supercoiling efficiency observed with the disulfide cross-linked gyrase. This suggests that both BMH and PDM may block DNA binding and cleavage, inhibit T-segment entry into the bottom cavity, or promote strand passage reversal. The former possibility can be eliminated since both complexes can perform quinolone- and Ca^{2+}-stabilized cleavage and DNA-stimulated ATP hydrolysis. This indicates that modification with BHM or PDM does not affect the enzyme's ability to bind and cleave a G segment or to present and capture a T segment. We have also shown that modification of gyrase with BMH or PDM does not block entry of the T segment into the bottom cavity. The truncated version of gyrase ($A64_2B_2$) catalyzes ATP-dependent strand passage in the presence of all three cross-linkers. Although the direction of strand passage performed by this complex is unclear, it can be inferred that the T segment must enter the cross-linked bottom cavity, either before or after strand passage. It is most likely that the low

level of supercoiling by BMH and PDM cross-linked gyrase is due to destabilization of T-segment binding within the bottom cavity. This is likely since Arg^{462} points directly into the cavity (Figure 1). After strand passage, the T segment is retained within the bottom cavity because exit is barred by the cross-linker. This may lead to strand passage reversal unless a second T segment is captured. The presence of the cross-linker may destabilize T-segment binding within the bottom cavity, promoting strand passage reversal before another T segment is captured. The longest cross-linker, BMH, is expected to destabilize T-segment binding the most, resulting in a low level of net strand passage. On the other hand, the shortest cross-linker, a disulfide bond, is expected to destabilize T-segment binding the least, resulting in a higher level of net strand passage (Figure 3 and Table 2).

ATP-Independent Relaxation: The T Segment Enters via the Bottom Gate of Gyrase, and Strand Passage Proceeds in the Reverse Direction to Supercoiling. Cross-linking the bottom dimer interface of gyrase completely abolishes ATP-independent relaxation activity; no net strand passage can be observed. However, G-segment binding is possible since the cross-linked complex can promote quinolone- and Ca^{2+}-stimulated cleavage of DNA, in the presence or absence of GyrA33. This suggests that T-segment entry is blocked by the cross-linker. In the absence of the cross-linker, the bottom dimer interface is free to open, allowing a segment of double-stranded DNA into the bottom cavity. Strand passage through a transient break in the G segment may then occur if it is energetically favorable.

Characterization of ATP-independent relaxation reveals that in the absence of ATP, DNA gyrase can only relax negatively supercoiled DNA (*30*, *31*). Relaxation of positively supercoiled DNA is strictly ATP-dependent and is thought to proceed in a manner analogous to that of supercoiling (*28*). In addition, we have found that ATP-independent relaxation is not performed by the truncated version of gyrase lacking the DNA wrapping domains. Together, these observations suggest that ATP-independent relaxation does not involve the random entry of a T segment through the bottom gate; otherwise, relaxation of positively supercoiled DNA would be possible since it is energetically favorable. Instead, this specificity may be explained in terms of the gyrase-mediated wrap. During DNA supercoiling, gyrase presents a T segment to the ATP-operated clamp, creating a positive node that is ready for inversion. Hence, after node inversion, the DNA must form a negative node (Figure 7); there are thus two possible wrapping conformations. In principle, the negatively wrapped conformation could present a T segment to the bottom dimer interface that is ready for entry. Upon entry, strand passage may occur, creating a positive node and resulting in relaxation. However, if the DNA substrate is positively supercoiled, this reaction would be energetically unfavorable and so would not proceed. Hence, ATP-independent relaxation can only be observed with negatively supercoiled DNA as a substrate.

Opening the Bottom Dimer Interface of $A64_2B_2$ Is Not Essential for ATP-Dependent Relaxation. In the absence of the GyrA33 domains, the resulting $A64_2B_2$ complex performs ATP-dependent relaxation, analogous to that of the conventional type II DNA topoisomerases, such as yeast topo II (*12*). The relaxation performed by $A64_2B_2$ is distributive, suggesting that a different G segment is used during each cycle. We have shown that locking the bottom dimer interface with a disulfide bond, PDM, or BMH does not block ATP-dependent relaxation by the $A64_2B_2$ complex. This suggests that opening of the bottom dimer interface is not essential during the $A64_2B_2$ cycle. Since relaxation requires ATP, this is likely to reflect T-segment capture via the ATP-operated clamp and passage through the G segment into the bottom cavity. If exit is blocked by the cross-linker, the A−B interface may open after strand passage, allowing dissociation of the G segment and the subsequent exit of the T segment through the DNA gate, bypassing the need for T-segment exit via the bottom gate. In the absence of a cross-linker, T-segment exit through the bottom gate cannot be ruled out, although since relaxation is distributive, the enzyme−DNA complex must dissociate prior to the next round of strand passage. It is not clear why the relaxation reaction is more efficient in the presence of the cross-linker. One possibility is that the cross-linker promotes complex dissociation when the T segment is retained in the bottom cavity, hence promoting enzyme turnover.

As an alternative to the above model, the complex may associate directly onto a pair of G and T segments, such that the T segment is located within the bottom cavity. This model also does not require opening of the bottom gate to allow T-segment exit. Despite this, the hypothesis is disfavored because it would require ATP-driven strand passage in the direction that is the opposite of the direction of that catalyzed by both gyrase and yeast topo II.

Role of the Bottom Dimer Interface in DNA Gyrase. Our results highlight the important role of the bottom dimer interface in DNA gyrase. The introduction of negative supercoils requires the capture of a DNA duplex by an ATP-operated clamp. The DNA is then passed through a transient break in a second DNA duplex held open by the DNA gate. After strand passage, we have shown that the T segment is expelled from the interior of the enzyme by the opening of a third gate (Figure 7). However, it seems that only two gates are essential to the strand passage event itself. So why does gyrase need this third bottom gate? This bottom dimer interface may confer stability to the enzyme, but another important role could be to sustain supercoiling. Since the introduction of negative supercoils is an energetically unfavorable process, the free energy of ATP hydrolysis is required to drive strand passage. The bottom gate may act as a physical barrier between the bound G segment and the expelled T segment to block the energetically favorable reversal of strand passage. However, it is clear that transient opening of this barrier is not tightly coupled to strand passage since it can open in the absence of ATP. This allows an ATP-independent form of relaxation in which the T segment enters through the open bottom gate and passes up through the enzyme, exiting via the open ATP-operated clamp (Figure 7). Whether the ability to reverse supercoiling in this manner represents an important in vivo role for gyrase is unknown. The level of supercoiling is controlled within the cell, with DNA topoisomerase I (topo I) implicated in ATP-independent relaxation. Topo I deletion mutants are not viable unless a compensating mutation in gyrase is present (*32*, *33*), implying that under normal circumstances the in vivo relaxation activity of gyrase is insignificant. It is possible that ATP-independent relaxation by gyrase may be an in vitro artifact, reflecting conditions under which the bottom dimer

interface is less stable. In vivo, bottom gate opening may be very tightly coupled to the strand passage mechanism, only opening transiently to enable exit of the T segment directly after strand passage.

In summary, we have found that supercoiling by DNA gyrase requires the bottom dimer interface to open to allow the exit of the T segment after strand passage. If the exit is blocked by a cross-linker, only a single strand passage event is possible. This is directly analogous to the situation with yeast topo II (*21*), suggesting that the two-gate model applies to all type II DNA topoisomerases (i.e., two different gates must open to allow T-segment entry and exit). It is likely that the two-gate model also applies to the truncated version of gyrase lacking the DNA wrapping domains. However, if the T segment is retained in the bottom cavity after strand passage by a cross-linker, the unstable $A64_2B_2$ complex dissociates from the DNA, bypassing the need for the bottom gate to open. The ATP-independent relaxation mechanism, unique to gyrase, is also blocked by cross-linking the bottom gate. No single-step strand passage is observed, implying that T-segment entry via the bottom gate is barred. This suggests that the ATP-independent relaxation mechanism is the reverse of the two-gate model. The T segment enters through the bottom dimer interface, followed by a reverse strand passage event and subsequent release through the open ATP-operated clamp.

ACKNOWLEDGMENT

We thank Sotiris Kampranis, Susan Hockings, and Mike Smyth for helpful suggestions and comments on the manuscript and Alison Howells for gifts of protein and DNA.

REFERENCES

1. Wang, J. C. (1998) *Q. Rev. Biophys. 31*, 107−144.
2. Wang, J. C. (1996) *Annu. Rev. Biochem. 65*, 635−692.
3. Lynn, R., Giaever, G., Swanberg, S., and Wang, J. C. (1986) *Science 233*, 647−648.
4. Ali, J. A., Jackson, A. P., Howells, A. J., and Maxwell, A. (1993) *Biochemistry 32*, 2717−2724.
5. Smith, C. V. (1998) Ph.D. Thesis, University of Leicester, Leicester, U.K.
6. Ali, J. A., Orphanides, G., and Maxwell, A. (1995) *Biochemistry 34*, 9801−9808.
7. Wigley, D. B., Davies, G. J., Dodson, E. J., Maxwell, A., and Dodson, G. (1991) *Nature 351*, 624−629.
8. Berger, J. M., Gamblin, S. J., Harrison, S. C., and Wang, J. C. (1996) *Nature 379*, 225−232.
9. Reece, R. J., and Maxwell, A. (1991) *J. Biol. Chem. 266*, 3540−3546.
10. Reece, R. J., and Maxwell, A. (1991) *Nucleic Acids Res. 19*, 1399−1405.
11. Morais Cabral, J. H., Jackson, A. P., Smith, C. V., Shikotra, N., Maxwell, A., and Liddington, R. C. (1997) *Nature 388*, 903−906.
12. Kampranis, S. C., and Maxwell, A. (1996) *Proc. Natl. Acad. Sci. U.S.A. 93*, 14416−14421.
13. Fass, D., Bogden, C. E., and Berger, J. M. (1999) *Nat. Struct. Biol. 6*, 322−326.
14. Maxwell, A. (1997) *Trends Microbiol. 5*, 102−109.
15. Willmott, C. J. R., Critchlow, S. E., Eperon, I. C., and Maxwell, A. (1994) *J. Mol. Biol. 242*, 351−363.
16. Drlica, K., and Zhao, X. (1997) *Microbiol. Mol. Biol. Rev. 61*, 377−392.
17. Reece, R. J., and Maxwell, A. (1989) *J. Biol. Chem. 264*, 19648−19653.
18. Lee, M. P., Sander, M., and Hsieh, T. (1989) *J. Biol. Chem. 264*, 21779−21787.
19. Roca, J., and Wang, J. C. (1992) *Cell 71*, 833−840.
20. Roca, J., and Wang, J. C. (1994) *Cell 77*, 609−616.
21. Roca, J., Berger, J. M., Harrison, S. C., and Wang, J. C. (1996) *Proc. Natl. Acad. Sci. U.S.A. 93*, 4057−4062.
22. Lindsley, J. E. (1996) *Proc. Natl. Acad. Sci. U.S.A. 93*, 2975−2980.
23. Hallett, P., Grimshaw, A. J., Wigley, D. B., and Maxwell, A. (1990) *Gene 93*, 139−142.
24. Thornton, J. (1981) *J. Mol. Biol. 151*, 261−287.
25. Richardson, J. (1981) *Adv. Protein Chem. 34*, 167−339.
26. Maxwell, A., and Gellert, M. (1984) *J. Biol. Chem. 259*, 14472−14480.
27. Tingey, A. P., and Maxwell, A. (1996) *Nucleic Acids Res. 24*, 4868−4873.
28. Bates, A. D., O'Dea, M. H., and Gellert, M. (1996) *Biochemistry 35*, 1408−1416.
29. Kampranis, S. C., Bates, A. D., and Maxwell, A. (1999) *Proc. Natl. Acad. Sci. U.S.A.* (in press).
30. Gellert, M., Mizuuchi, K., O'Dea, M. H., Itoh, T., and Tomizawa, J. (1977) *Proc. Natl. Acad. Sci. U.S.A. 74*, 4772−4776.
31. Gellert, M., Fisher, L. M., Ohmori, H., O'Dea, M. H., and Mizuuchi, K. (1980) *Cold Spring Harbor Symp. Quant. Biol. 45*, 391−398.
32. DiNardo, S., Voekel, K., and Sternglanz, R. (1982) *Cell 31*, 43−51.
33. Pruss, G., Manes, S., and Drlica, K. (1982) *Cell 31*, 35−42.

BI9912488